

Observation of quantum equilibration in dilute Bose gasesLinxiao Niu (牛临潇),¹ Pengju Tang (唐鹏举),¹ Baoguo Yang (杨保国),¹ Xuzong Chen (陈徐宗),¹
Biao Wu (吴飙),^{2,3,4,5,*} and Xiaoji Zhou (周小计)^{1,†}¹*School of Electronics Engineering and Computer Science, Peking University, Beijing 100871, China*²*International Center for Quantum Materials, School of Physics, Peking University, Beijing 100871, China*³*Collaborative Innovation Center of Quantum Matter, Beijing 100871, China*⁴*Wilczek Quantum Center, Department of Physics and Astronomy, Shanghai Jiao Tong University, Shanghai 200240, China*⁵*Synergetic Innovation Center for Quantum Effects and Applications, Hunan Normal University, Changsha 410081, China*

(Received 7 May 2016; published 5 December 2016)

We investigate experimentally the dynamical relaxation of a nonintegrable quantum many-body system to its equilibrium state. A Bose-Einstein condensate is loaded into the first excited band of an optical lattice and let to evolve up to a few hundreds of milliseconds. Signs of quantum equilibration are observed. There is a period of time, roughly 40 ms long, during which both the aspect ratio of the cloud and its momentum distribution remain constant. In particular, the momentum distribution has a flat top and is not a Gaussian thermal distribution. After this period, the cloud becomes classical as its momentum distribution becomes Gaussian.

DOI: [10.1103/PhysRevA.94.063603](https://doi.org/10.1103/PhysRevA.94.063603)**I. INTRODUCTION**

The second law of thermodynamics states that the entropy of an isolated system never decreases [1]. When applied to quantum systems, the second law implies that an isolated quantum system will dynamically relax to an equilibrium state that has a maximized entropy. Many physicists including Pauli and Schrödinger had attempted to understand this law quantum mechanically [2]. Von Neumann was clearly the most successful as he proved both quantum ergodic theorem and quantum H-theorem [3,4]. According to these two theorems, most of the nonintegrable quantum systems, which are ubiquitous in nature [5], will indeed relax dynamically to an equilibrium state, where the macroscopic observables fluctuate only slightly and the entropy is maximized with small fluctuations. These two theorems have now been improved and put in a more transparent framework and on a firmer footing [6,7].

Experimental observation of the dynamical relaxation of an isolated quantum system had been almost impossible since isolated quantum systems are very hard to prepare in experiments. This situation was changed with the realization of Bose-Einstein condensation (BEC) in dilute atomic gases [8]. A BEC in such an experiment has no physical contact with a heat bath as it is held either in a magnetic or an optical trap. As demonstrated in interference and vortex experiments [9,10] and also in our recent experiment [11], a BEC can stay in a pure quantum state or the BEC can be regarded as an isolated quantum system up to a few hundred milliseconds. This shows that it is now experimentally feasible to study the dynamical relaxation of an isolated quantum system. Such a possibility has generated a great deal of theoretical interests. Along with many theoretical works [12–18], there have already been experimental studies on this issue. However, almost all of the experiments are focused on one-dimensional integrable quantum systems [19–23]. To the best of our knowledge, the dynamical relaxation of a nonintegrable quantum system was only studied

in Refs. [24–26] with the focus on quantum turbulence. As integrable systems are rare and almost all interacting systems in nature are nonintegrable [5], it is more important to study the dynamical relaxation of nonintegrable quantum systems.

In this work we study experimentally the dynamical relaxation of an isolated nonintegrable quantum system, which is a BEC loaded into the first excited band of an optical lattice. The BEC is then allowed to evolve up to 400 ms. The aspect ratio of the BEC cloud after free expansion is measured, and found to oscillate initially and then becomes constant during a time window between roughly 35 ms and 50 ms (see Fig. 1). For convenience, we refer to this time window as plateau phase. During the plateau phase, the momentum distribution of the atomic cloud remains largely unchanged, and has a flat top such that it cannot be fitted with any known thermal distribution. This observation strongly indicates that a possible quantum equilibrium is reached. The length of this plateau phase is around 40 ms for an optical lattice of $20E_r$, and it increases with the strength of optical lattice. After the plateau, the momentum distribution of the BEC becomes Gaussian-like and the oscillations in the aspect ratio are resumed with a frequency that is twice that of the trapping frequency. The system eventually reaches the classical thermal equilibrium, where the momentum distribution of the BEC is Gaussian. The nonintegrability of our system, a BEC in an optical lattice, is indicated by the dynamical instability found in this system both theoretically [27,28] and experimentally [29].

The article is organized as follows. In Sec. II, we briefly describe our experimental setup, and report that the evolution of our BEC system undergoes three stages. In Sec. III, we give a detailed description and an analysis of the second stage, where the quantum equilibrium is reached. In Sec. IV, we describe the third stage, where the classical thermalization is finally reached. We conclude in Sec. V.

II. EXPERIMENTAL SETUP

The experimental setup is similar to our previous work [30]. A nearly pure condensate of about 1.5×10^5 ^{87}Rb atoms is obtained in our hybrid optical-magnetic trap whose harmonic

*wubiao@pku.edu.cn

†xjzhou@pku.edu.cn

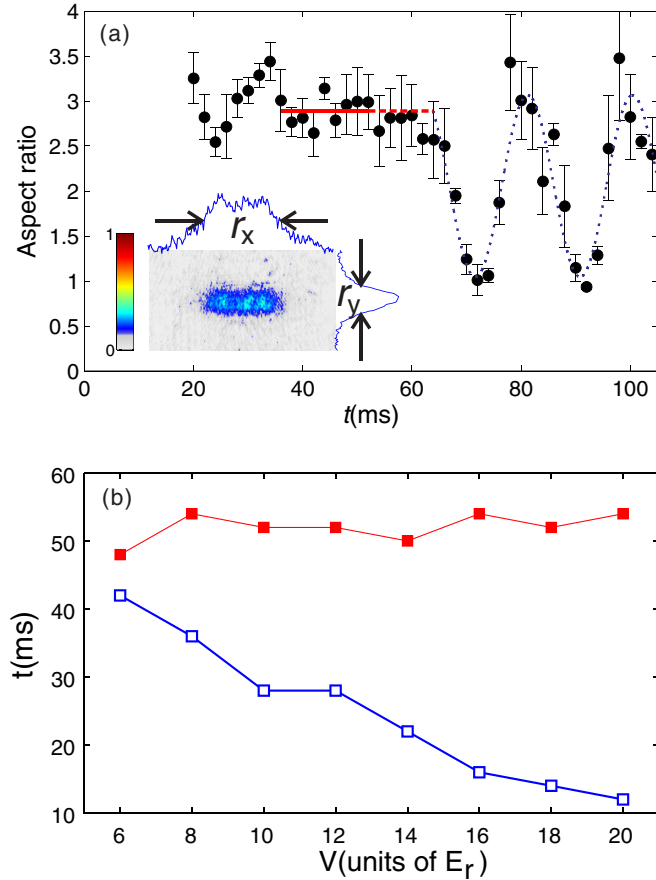


FIG. 1. (a) Aspect ratios of the atomic cloud at different holding times with the lattice strength $V = 8E_r$. The TOF image at 50 ms is shown in the inset to show how the aspect ratio is extracted. Each point is the average over five experiments and the error bar is the standard error. The red solid line indicates the plateau during which the aspect ratio remains constant while the red dashed line shows the transition period between two stages. (b) The starting (blue) and ending times (red) of the plateau for different lattice strengths.

trapping frequencies are $(\omega_x, \omega_y, \omega_z) = 2\pi \times (28, 55, 65)$ Hz. A one-dimensional optical lattice is formed along the x direction by retroreflecting a laser beam with wavelength $\lambda = 852$ nm. The lattice constant is then $a = \lambda/2 = 426$ nm. The lattice depth is expressed in units of recoil energy $E_r = \frac{\hbar^2 k^2}{2m}$ with $k = 2\pi/\lambda$. The condensate is quickly loaded into the p band (first excited band) of the optical lattice by using a series of pulsed optical lattices. The pulses are tens of microseconds wide and consist of two sets whose lattice sites are shifted in the \hat{x} axis by $a/4$. The details of our method can be found in Ref. [30]. The condensate prepared in such a way has a narrow distribution of quasimomentum around $q = 0$. A lot of interesting physics has been studied both theoretically and experimentally for a BEC in the p band [31–35], with a narrow quasimomentum distribution or fully occupied. In this work we focus on the dynamical relaxation of a BEC in the p band.

We hold the condensate in the p band for a period of time t . Then all the potentials are switched off and the atomic cloud is released. After a 28 ms free expansion, we take the time-of-flight (TOF) absorption image, which shows the momentum

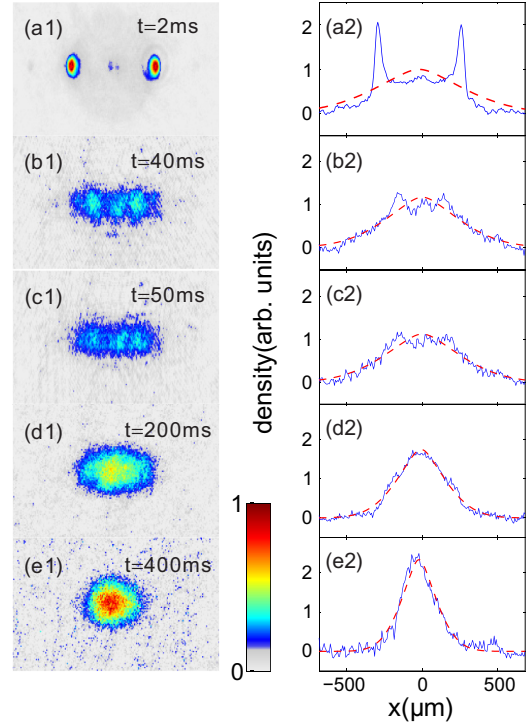


FIG. 2. The TOF images (left column) and the corresponding integrated one-dimensional distribution (right column) at five typical times: $t = 2$ ms, $t = 40$ ms, $t = 50$ ms, $t = 200$ ms, and $t = 400$ ms. The red dashed lines in the right column are the best thermal distribution fit. $V = 8E_r$.

distribution of the atomic cloud. TOF images at five typical holding times are shown in Fig. 2. Initially there are two peaks at $q = \pm\hbar k$, clearly indicates that the condensate is in the p band [35]. As the evolution goes on, these two peaks start to disappear and a central peak with a flat top emerges around tens of milliseconds, and the distribution stays unchanged for a period of time, an indication that the quantum equilibrium is reached. At 200 ms, the momentum distribution becomes Gaussian-like, a signal of the classical thermal distribution. At 400 ms, we not only observe the thermal distribution but also the overall cloud shape becomes circular, implying that the classical thermal equilibrium is reached [24].

We have analyzed the TOF images in detail, and find that the whole evolution can be divided into three typical stages. There is an initial oscillation period roughly before 20 ms and this stage is characterized by the two prominent Bragg peaks and oscillations in the aspect ratio of the BEC cloud. The detailed analysis of this stage has been done in our previous work [30]. The second stage follows immediately and we call it plateau phase. In the plateau phase, the system enters into a stable state, where all the quantities that we can and have measured remain almost constant, indicating that a kind equilibrium is reached. This plateau phase always ends around 50 ms no matter how strong the optical lattice is (see Fig. 1), which is much shorter than the decoherence time 125 ms due to the thermal fraction (details are given later). This means that the atomic cloud is still in a quantum pure state during this stage and the observed equilibrium is of quantum nature. After the second stage, the aspect ratio of the BEC cloud begins to oscillate again but

with a frequency that is twice the trapping frequency. The oscillations eventually die out. At the third stage, all the TOF images can be well fit by a Gaussian function. At this final stage the system is in a mixed state due to inevitable experimental noise and finally becomes classically thermalized.

III. QUANTUM EQUILIBRIUM

According to von Neumann [3,4] and others [6,7], a non-integrable quantum many-body system starting from a well-behaved pure state, such as a Gaussian wave packet and a Bloch state, will eventually evolve dynamically into an equilibrium state, which looks intuitively rather random or irregular. As a result, there are two stages of dynamical evolution. In the first stage, which is usually short and characterized by a relaxation time, the quantum system undergoes a certain type of coherent dynamics, which will quickly be destroyed by dephasing. To see this clearly, let us write the dynamics of a quantum system in its general form

$$|\psi(t)\rangle = \sum_n c_n e^{-iE_n t/\hbar} |E_n\rangle, \quad (1)$$

where $|E_n\rangle$ is the system's energy eigenstate with eigenenergy E_n and coefficient c_n determined by the initial condition. For a nonintegrable quantum system, the structure of its energy eigenvalues E_n is very similar to the one of a random matrix [5]. As a result, the phases $e^{-iE_n t/\hbar}$ will quickly be scrambled as t increases and the dephasing occurs. Such dephasing causes the quantum system to equilibrate [3,4,6,7]. In this way, the quantum system enters the second stage, where besides small fluctuations all the observables become constant.

The above theoretical discussion is for a quantum system ideally isolated from the environment and the quantum system is still in a pure state even in the quantum equilibrium stage. In a real experiment, the quantum system is always coupled to an environment, which can drive a quantum pure state into a mixed state. If the coupling is strong, the second quantum equilibrium stage may never happen as the quantum system can quickly be driven into a mixed state and becomes classical. When the coupling is weak, the second stage can survive for a period of time before entering the third stage, where the system evolves into a mixed state and eventually equilibrates classically.

In our experiment, the coupling to the environment is weak enough that we have indeed observed all the three stages. We use t_1 to denote the transition time that the system goes from the first to the second stage and t_2 the time that the third stage begins. In the first stage coherent oscillations with decay amplitude are observed along with other dynamical features. We have analyzed this stage in detail in Ref. [30]. We shall concentrate on the second and the third stages.

We first characterize the TOF images of the BEC quantitatively using the aspect ratio of the cloud. We calculate, r_x and r_y , the full widths at half maximum (FWHM) of the atomic cloud in the TOF images along the x and y axes, respectively. The FWHM in each direction is obtained by integrating the two-dimensional atom distribution in the perpendicular direction to get a one-dimensional momentum distribution and then counting pixels with atom number higher than half of the maximum value. The aspect ratio is then $r = r_x/r_y$. We have

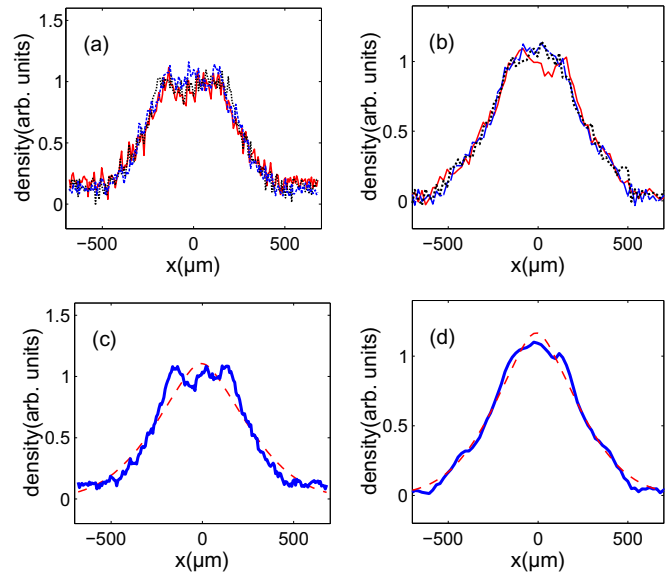


FIG. 3. The momentum distribution at the beginning (red solid line), in the middle (black dotted line), and at the end (blue dashed line) of the quantum equilibrium plateau for (a) $8E_r$ and (b) $14E_r$. The momentum distribution averaged over the entire equilibrium plateau is shown in (c) for $8E_r$ and (d) for $14E_r$ with solid blue lines while the thermal fitting is shown with red dashed lines.

plotted how the aspect ratio changes with time for the case of $V = 8E_r$ in Fig. 1(a), where each point is the average over five experiments with error bars given by the standard deviation. There is clearly a plateau in this figure during which the aspect ratio remains largely constant. Note that the ratio of this plateau is about 3, which is far away from 1, the aspect ratio of a thermal cloud [see Fig. 2(e1)]. This is one of the indications that the cloud is still quantum during this plateau phase.

In Fig. 3, we have plotted the momentum distributions at different times of this plateau. To demonstrate that the distribution changes little over the plateau, the momentum distributions at the beginning, in the middle, and at the end of the plateau are shown in Figs. 3(a) and 3(b) for the lattice depths of $8E_r$ and $14E_r$, respectively. Besides some minor fluctuations, the distributions at different times are clearly the same. To reduce the background noise, each line is the average over five experiments with the same holding time. Furthermore, we have plotted in Figs. 3(c) and 3(d) the averaged momentum distribution over the entire plateau for $V = 8E_r$ and $V = 14E_r$, respectively. Similar to the distributions at individual times, these two averaged distributions have a flat top and cannot be fitted well with a Gaussian. All these features strongly indicate that the system has reached a steady state, which can at least be called quasiequilibrium. Since the momentum distribution of this state has a rather flat top and cannot be fitted with the thermal Gaussian distribution, we argue along with other features that this is quantum equilibrium.

The two transition times t_1 and t_2 can be extracted. Our criterion considers both the aspect ratio r and the momentum distribution. We first determine t_1 and t_2 by requiring the aspect ratio r fluctuates less than 10% of the average value. The average value is also modified when a new point is included. For lattices with strength bigger than $14E_r$, the

criterion is changed to 20% when the time span is longer than 20 ms, as the fluctuations of the experimental results are larger for higher lattice depths. Then time t_2 is adjusted by looking into the momentum distribution. For example, in the case of $V = 8E_r$, we have $t_1 = 36$ ms and $t_2 = 62$ ms by just considering the fluctuation of r . However, we find that the momentum distribution begins to change gradually from a flat top to a Gaussian one starting at $t = 52$ ms. As a result, we set $t_2 = 52$ ms, instead of 62 ms. For other lattice depths, this phenomenon is also existed, and each t_2 is roughly reduced by 10 ms after considering this effect.

These two times are plotted in Fig. 1(b) as a function of lattice strength V with t_1 as blue filled squares and t_2 as red open squares. The transition time t_1 is seen decreased with the lattice strength, indicating that the stronger lattice renders the cloud to quantum equilibrium faster. This is quite reasonable: If we use the dynamical instability to characterize how strong the chaos of the system is, it is known in literature that a BEC in an optical lattice is more chaotic for stronger lattice [27]. Usually more chaotic systems have shorter relaxation times.

The other transition time t_2 remains almost constant around 52 ms. This observation is also consistent with our basic understanding. Our experimental system is weakly coupled to an environment, which includes thermal atoms [39], fluctuations of laser field [36], and inelastic scattering of photons [37,38]. These noises can eventually destroy the quantumness of the system and turn it from a pure state to a mixed state. As this coupling to the environment is insensitive to the details of the BEC system, one expects that t_2 should be independent of the lattice strength. This is indeed what we have observed.

Overall, we have observed in this stage an equilibrium state. It is clearly not classical for two reasons: (i) the aspect ratio is 3 whereas it is 1 for a thermal cloud; (ii) the momentum distribution has a flat top. We argue that this equilibrium state is of quantum nature as it exists only for a short time period and roughly ends at 52 ms. We have estimated the environmental effects. The fractional thermal cloud dominates, and the relaxation time due to the thermal collision is about 125 ms [39], which is much longer than $t_2 \approx 52$ ms. The effects of laser field fluctuations and the inelastic scattering of photons would induce a decay on a timescale of several seconds, which is orders of magnitude longer than t_2 .

Another strong evidence that our system is still in a pure quantum state in the second stage comes directly from our own experiment in Ref. [11]. The experimental setup is the same. The only difference is that the BEC is loaded into the f band in Ref. [11], where quantum coherent oscillations similar to Bloch oscillations were observed up to 60 ms. Quantum equilibration was not observed in Ref. [11]. The reason is that the kinetic energy dominates the high bands and the interaction can be ignored so that the system is integrable.

In literature there are also a great deal of evidence that the BEC can remain in pure quantum state up to tens of milliseconds. In Ref. [24], the BEC was shaken up to 60 ms and quantum turbulence was still observed. The typical lifetime of a BEC vortex is around 500 ms [10]; this means that the phase coherence of a BEC can be up to 500 ms.

According to von Neumann [3,4], the equilibrium state we observed in the second stage is caused by the nonintegra-

bility of the system. Specifically, for our BEC system, the nonintegrability comes from the interaction between atoms. The collisions between the atoms can deplete the p band and render the atoms to the s band and higher bands or lateral motion. The reverse process can also occur. At the end, these two processes can balance out and our BEC system reaches equilibrium.

The details of the quantum dynamical evolution in the second stage can in principle be described by the many-body Schrödinger equation. However, at present there is no tractable way to solve this equation for our system, which is initially loaded to the $q = 0$ state of the p band. The mean-field Gross-Pitaevskii equation can only describe the early moments of the dynamics before the Ehrenfest time (much shorter than t_1) [40] due to the existence of dynamical instability [28].

IV. CLASSICAL THERMALIZATION

The third stage of the evolution starts around 60 ms, and is characterized by its Gaussian momentum distribution. Interestingly, the aspect ratio of the cloud starts to oscillate again in this stage but with a different frequency. These oscillations last for a long time until the system eventually reaches the classical equilibrium around a few hundreds of milliseconds. As the cloud with r_y is roughly constant, the width r_x oscillates in an identical fashion with r . The oscillations of the aspect ratio r for the case of $V = 8E_r$ are shown in Fig. 4(a). They can be well fitted with slowly decaying sine

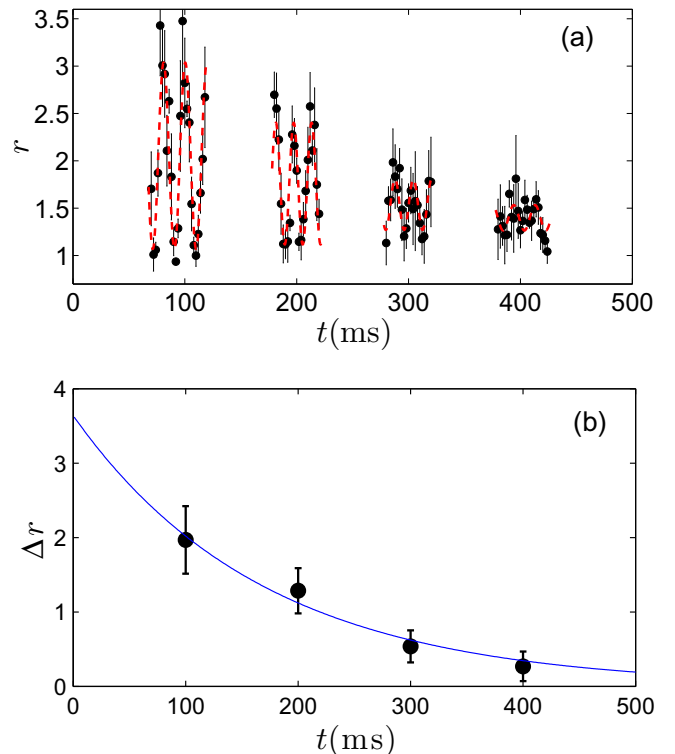


FIG. 4. (a) Oscillations of the aspect ratio r . The dashed line is a theoretical fitting. The oscillation frequency is about twice the trapping frequency along the direction of optical lattice. (b) Decay of amplitude of the oscillations. The solid line represents an exponential fit. $V = 8E_r$.

functions. Through the fitting, we find the oscillation frequency is $\omega = 2\pi \times 55.3 \pm 0.49$ Hz. This is approximately twice of the trapping frequency $\omega_x = 2\pi \times 28$ Hz. This frequency doubling is independent of the lattice strength.

This oscillation phenomenon is of classical nature and can be explained as follows. A gas in a harmonic potential can be regarded as a gas of harmonic oscillators with the same frequency. As a result, according to the law of equipartition of energy, its kinetic energy must be equal to its potential energy at equilibrium. In our experiment, when the quantum gas loses its coherence and becomes classical at time t_2 , it is yet to reach equilibrium with the harmonic trapping potential. As each atom in the gas oscillates in the trapping potential, the momentum distribution of this gas will oscillate accordingly with a doubled frequency. The reason is that after half of the harmonic oscillation cycle, each atom would change the direction of its momentum in \hat{x} axis while maintaining the magnitude. Due to the symmetry of the system, the overall momentum distribution would have restored the initial state.

As the atomic cloud is not ideally isolated in experiments and the trap is not perfectly harmonic, it will eventually equilibrate with the trapping potential. This is demonstrated by the damping of the oscillation amplitude of the aspect ratio Δr as shown in Fig. 4(b). A numerical fitting shows that the damping follows an exponential form $A_0 e^{-t/t_d}$ with $t_d = 169.8 \pm 28.7$ ms. Such a long relaxation time shows that the system is well isolated and is an indirect indication that the equilibration observed in the plateau is of quantum nature.

For lattice depth of $8 E_r$ the aspect ratio of the atomic cloud becomes constant around 400 ms. For a deeper lattice, the system would reach thermal equilibrium faster.

V. CONCLUSION

In sum, we have studied experimentally the dynamical relaxation of a nonintegrable quantum system by loading a BEC into the second band of the optical lattice. By following its time evolution, we have observed a quantum equilibrium state, which is characterized by a constant non-Gaussian momentum distribution. Our study here has presented a preliminary experimental test of the two fundamental theorems proved by von Neumann in his pioneering work [3,4]. Much more is needed in order to clarify many aspects of this dynamical relaxation. For example, what else can we measure to characterize the quantum equilibrium? And, ultimately, can we measure the quantum entropies for quantum pure states defined by von Neumann [3,4] or in Ref. [7]?

ACKNOWLEDGMENTS

We acknowledge helpful discussion with Hongwei Xiong. This work is supported by the National Key Research and Development Program of China (Grant No. 2016YFA0301501), the NSFC (Grants No. 61475007, No. 1274024, No. 11334001, No. 1429402, No. 91336103, and No. 11274022), and the National Basic Research Program of China (Grants No. 2013CB921903 and No. 2012CB921300).

-
- [1] K. Huang, *Statistical Mechanics* (Wiley, New York, 1987).
 - [2] S. Goldstein, J. Lebowitz, R. Tumulka, and N. Zanghi, *Eur. Phys. J. H* **35**, 173 (2010).
 - [3] J. von Neumann, *Z. Phys.* **57**, 30 (1929).
 - [4] J. von Neumann, *Eur. Phys. J. H* **35**, 201 (2010).
 - [5] M. C. Gutzwiller, *Chaos in Classical and Quantum Mechanics* (Springer-Verlag, New York, 1990).
 - [6] P. Reimann, *Phys. Rev. Lett.* **101**, 190403 (2008).
 - [7] X. Han and B. Wu, *Phys. Rev. E* **91**, 062106 (2015).
 - [8] M. H. Anderson, J. R. Ensher, M. R. Matthews, C. E. Wieman, and E. A. Cornell, *Science* **269**, 198 (1995).
 - [9] M. R. Andrews, C. G. Townsend, H. Miesner, D. S. Durfee, D. M. Kurn, and W. Ketterle, *Science* **275**, 637 (1997).
 - [10] K. W. Madison, F. Chevy, W. Wohlleben, and J. Dalibard, *Phys. Rev. Lett.* **84**, 806 (2000).
 - [11] Z. Wang, B. Yang, D. Hu, X. Chen, H. Xiong, B. Wu, and X. Zhou, *Phys. Rev. A* **94**, 033624 (2016).
 - [12] S. Goldstein, J. L. Lebowitz, R. Tumulka, and N. Zanghi, *Phys. Rev. Lett.* **96**, 050403 (2006).
 - [13] S. Popescu, A. J. Short, and A. Winter, *Nature Phys.* **2**, 754 (2006).
 - [14] N. Linden, S. Popescu, A. J. Short, and A. Winter, *Phys. Rev. E* **79**, 061103 (2009).
 - [15] A. J. Short, *New J. Phys.* **13**, 053009 (2011).
 - [16] V. Yukalov, *Laser Phys. Lett.* **8**, 485 (2011).
 - [17] Q. Zhuang and B. Wu, *Phys. Rev. E* **88**, 062147 (2013).
 - [18] Q. Zhuang and B. Wu, *Laser Phys. Lett.* **11**, 085501 (2014).
 - [19] T. Kinoshita, T. Wenger, and D. S. Weiss, *Nature (London)* **440**, 900 (2006).
 - [20] M. Gring, M. Kuhnert, T. Langen, T. Kitagawa, B. Rauer, M. Schreitl, I. Mazets, D. A. Smith, E. Demler, and J. Schmiedmayer, *Science* **337**, 1318 (2012).
 - [21] D. A. Smith, M. Gring, T. Langen, M. Kuhnert, B. Rauer, R. Geiger, T. Kitagawa, I. Mazets, E. Demler, and J. Schmiedmayer, *New J. Phys.* **15**, 075011 (2013).
 - [22] M. Schreiber, S. S. Hodgman, P. Bordia, H. P. Lüschen, M. H. Fischer, R. Vosk, E. Altman, U. Schneider, and I. Bloch, *Science* **349**, 842 (2015).
 - [23] P. Bordia, H. P. Lüschen, S. S. Hodgman, M. Schreiber, I. Bloch, and U. Schneider, *Phys. Rev. Lett.* **116**, 140401 (2016).
 - [24] E. A. L. Henn, J. A. Seman, G. Roati, K. M. F. Magalhães, and V. S. Bagnato, *Phys. Rev. Lett.* **103**, 045301 (2009).
 - [25] M. Caracanhas, A. L. Fetter, G. Baym, S. R. Muniz, and V. S. Bagnato, *J. Low Temp. Phys.* **170**, 133 (2013).
 - [26] J. A. Seman, E. A. L. Henn, R. F. Shiozaki, G. Roati, F. J. Poveda-Cuevas, K. M. F. Magalhães, V. I. Yukalov, M. Tsubota, M. Kobayashi, K. Kasamatsu, and V. S. Bagnato, *Laser Phys. Lett.* **8**, 691 (2010).
 - [27] B. Wu and Q. Niu, *Phys. Rev. A* **64**, 061603(R) (2001).
 - [28] Y. Xu, Z. Chen, H. Xiong, W. V. Liu, and B. Wu, *Phys. Rev. A* **87**, 013635 (2013).
 - [29] L. Fallani, L. DeSarlo, J. E. Lye, M. Modugno, R. Saers, C. Fort, and M. Inguscio, *Phys. Rev. Lett.* **93**, 140406 (2004).
 - [30] D. Hu, L. Niu, B. Yang, X. Chen, B. Wu, H. Xiong, and X. Zhou, *Phys. Rev. A* **92**, 043614 (2015).

- [31] X. Li, Z. Zhang, and W. V. Liu, *Phys. Rev. Lett.* **108**, 175302 (2012).
- [32] W. V. Liu and C. Wu, *Phys. Rev. A* **74**, 013607 (2006).
- [33] T. Kock, C. Hippler, A. Ewerbeck, and A. Hemmerich, *J. Phys. B* **49**, 042001 (2016).
- [34] M. Ölschläger, T. Kock, G. Wirth, A. Ewerbeck, C. M. Smith, and A. Hemmerich, *New J. Phys.* **15**, 83041 (2013).
- [35] G. Wirth and A. Hemmerich, *Nature Phys.* **7**, 147 (2011).
- [36] H. Pichler, J. Schachenmayer, A. J. Daley, and P. Zoller, *Phys. Rev. A* **87**, 033606 (2013).
- [37] H. Pichler, A. J. Daley, and P. Zoller, *Phys. Rev. A* **82**, 063605 (2010).
- [38] F. Gerbier and Y. Castin, *Phys. Rev. A* **82**, 013615 (2010).
- [39] T. Nikuni and A. Griffin, *Phys. Rev. A* **65**, 011601 (2001).
- [40] X. Han and B. Wu, *Phys. Rev. A* **93**, 023621 (2016).